Journal of Structural Geology, Vol. 14, No. 5, pp. 591 to 604, 1992
Printed in Great Britain

0191-8141/92 $05.00+0.00

The influence of deformation on the formation of axial-planar leucosomes and the segregation of small melt bodies within the migmatitic Napperby Gneiss, central Australia

MARTIN HAND and PAUL H. G. M. DIRKS*

Department of Geology, University of Melbourne, Parkville, Victoria 3052, Australia

(*Received* 23 *January* 1991; *accepted in revised form* 3 *December* 1991)

Abstract—In the Napperby Gneiss, central Australia, a distinctive group of elongate leucosomes occurs along the axial planes of mesoscopic crenulations that have harmonic, two-dimensional, kink band-like geometries. The leucosomes truncate a fabric defined by biotite, quartz, K-feldspar, plagioclase ± sillimanite and are chiefly composed of K-feldspar and quartz with or without plagioclase. They are characterized by accessory garnet or aggregates of intergrown ilmenite and magnetite produced during the melting reactions; bi + plag + q + sill = g + ksp + melt, and bi + plag + q ± ru = ilm + mt + ksp + melt. The absence of garnet and intergrown ilmenite–magnetite aggregates in the gneiss surrounding the crenulation zones indicates that these melting reactions preferentially occurred in the deformation zones in spite of a homogeneous distribution of reactant phases in the gneiss. This means that strain partitioning and partial melting are coupled processes, in which the garnet- and ilmenite–magnetite-producing melt reactions initially occurred in high strain zones where the melting reaction activation energy was first overstepped. This was a consequence of an additional strain-induced, matrix-free energy component on top of the temperature effect. Once reaction product-nucleation had occurred, the deformation zones became the sites for continued melting, which was energetically favoured over nucleating garnet and ilmenite–magnetite elsewhere.

The melt reactions producing garnet and ilmenite–magnetite resulted in the formation of grain-supported leucosomes with a higher melt component than the surrounding gneiss, and the leucosomes were therefore relatively incompetent. In a differential stress field, diffusional processes will cause elongation of the leucosome in a plane normal to σ_1, parallel to the axial planes of folds. If sufficient melting has occurred, an interconnected leucosome network will result, creating a potentially important, buoyancy-driven, melt drainage system.

In the Napperby Gneiss, interconnected, leucosome-bearing crenulation zones are mostly vertical, which is an ideal orientation for buoyancy-driven, diffusive melt migration. However, melt segregations remained small due to a melt-impermeable, lithological boundary overlying the gneiss.

INTRODUCTION

MUCH experimental work has been done on the various melt processes that play a role in anatexis (Mehnert *et al.* 1973, Arzi 1978, van der Molen & Paterson 1979, Thompson 1982, Vielzeuf & Holloway 1988). Likewise, many theoretical and experimental studies have discussed the behaviour of melt in model migmatite (Watson 1982, McKenzie 1984, Grant 1985, Jurewicz & Watson 1985, von Bargen & Waff 1986, Wickham 1987). Most of this work deals with mafic systems and applies to hydrostatic conditions and so is not easily applied to natural systems. Edelman (1973) described geometric relationships between melt bodies and fold structures, and Wickham (1987) and McLellan (1988) limited their discussion to the influence of extensional and brittle structures on the segregation of melt, without considering the interplay between plastic deformational processes and melting. In this paper we present detailed field observations from the Napperby Gneiss, central Australia, and attempt to demonstrate the relationships and mutual influences that exist between plastic deformational processes, strain localization and the generation, segregation and mobilization of melt.

The Napperby Gneiss is a quartzofeldspathic gneiss which occurs along the southern flank of the Reynolds Range, central Australia (Fig. 1), and belongs to a suite of rocks that were metamorphosed and deformed during a mid-Proterozoic event. Dirks & Wilson (1990) considered this to be a single event (*D*II–*M*II) that overprinted an earlier event (*D*I–*M*I). However, subsequent high precision zircon dating using the SHRIMP ion microprobe (Hand unpublished data) suggests the *D*II–*M*II event may consist of several closely spaced but not necessarily related events (Fig. 2). Peak metamorphic conditions varied from upper-amphibolite facies in the south (~680°C, 4.1 kbar) to granulite facies in the north (~740°C, 4.1 kbar, Dirks 1990, Clarke & Powell 1991, Dirks *et al.* 1991). A NW-trending, upright regional gneissic foliation, S_{II_2} has been folded along D_{II_3} crenulation zones that have distinct, two-dimensional, kink band-like geometries. Ion probe zircon dating (Hand unpublished data) indicates a time interval of 90–120 Ma between the formation of S_{II_2} and the D_{II_3} crenulation zones (Fig. 2). At mid-crustal pressures, such a time interval suggests that the S_{II_2} fabric and the D_{II_3} crenulation zones are likely to represent two separate structural–metamorphic events (Sandiford & Powell 1991).

The leucosomes being considered here occur exclusively within the D_{II_3} crenulation zones in the Napperby Gneiss and will be referred to as D_{II_3} leucosomes. They comprise two distinct types, both oriented parallel to the

* Present address: Institute of Earth Sciences, University of Utrecht, Utrecht 3508 TA, The Netherlands.

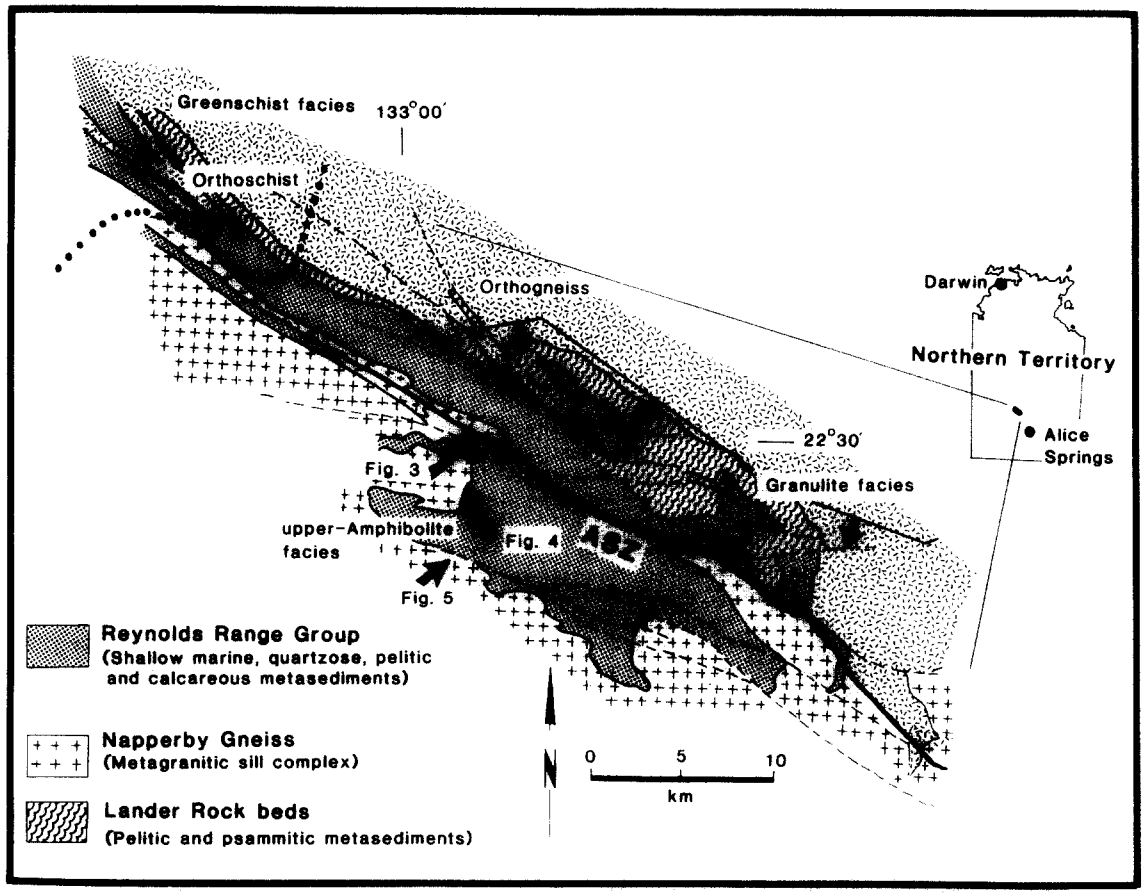

Fig. 1. Locality map of the Reynolds Range, Arunta Block, central Australia. The distributions of the Napperby Gneiss and the Reynolds Range Group, which was intruded by the granitic precursor to the Napperby Gneiss, are indicated. Also indicated are the generalized metamorphic zones, the heavy dotted line marking the rapid transition from greenschist facies to upper amphibolite facies rocks. The region bounded by the arrowed line and the ASZ (Aileron shear zone) comprises granulite grade rocks. The ASZ separates granulite facies Napperby Gneiss to the northeast from upper-amphibolite facies gneiss to the southwest. The localities of Figs. 3, 4 and 5 are also shown.

axial surfaces of individual crenulations: (1) leucosomes containing coarse-grained garnet (up to 15 cm) or intergrowths of ilmenite–magnetite; and (2) coarse-grained leucosomes without mafic phases. Earlier leucosomes parallel to the regional SII_2 gneissic fabric are easily distinguished from the DII_3 leucosomes, and in comparison are volumetrically insignificant. These earlier leucosomes are fine-grained, never contain garnet or ilmenite–magnetite, and are clearly folded by the DII_3 crenulations and transected by the DII_3 leucosomes. Garnet and ilmenite–magnetite blasts within the younger leucosomes are thought to represent solid, relatively immobile products of melting reactions (e.g. Powell & Downes 1990). The abundance of leucosome and the exclusive occurrence of these solid phases in the DII_3 crenulation zones imply a relationship between the occurrence of garnet- and ilmenite–magnetite-producing melt reactions and deformation. The identical mode of occurrence of coarse-grained, non-garnet- or ilmenite–magnetite-bearing leucosomes within some DII_3 crenulation zones strongly suggests that other melting reactions were also localized along these structures. This suggests that a general relationship potentially exists between deformation and melting. The DII_3 leucosomes along the crenulations locally merge with intrusive, metre-scale microgranites, implying that DII_3 structures also played an important role in the mobilization and segregation of melt. The three processes of strain localization, melt generation and melt segregation are clearly not mutually exclusive here, and an understanding of their relationship is essential in understanding magma generation in the Napperby Gneiss and other active tectonic settings. The occurrence of similar leucosomes and leucosome geometries within ductile structures in a number of migmatite terranes (e.g. McLellan 1988, Sisson & Hollister 1988, Norman & Clarke 1990, Passchier *et al.* 1990, Nijland & Senior 1991) indicates that the inferred processes may represent an important mechanism by which melts can be generated and segregated.

DESCRIPTION OF THE DII_3 LEUCOSOMES

Structural setting

The vast majority of leucosomes in the the Napperby Gneiss occur within decimetre-scale, DII_3 crenulation zones that are the mesoscopic expression of large-scale (100–1000 m), SE-trending, DII_3 monoclinal folds which deform the SII_2 gneissic fabric (Figs. 3 and 4) (Dirks & Wilson 1990). The crenulation zones are de-

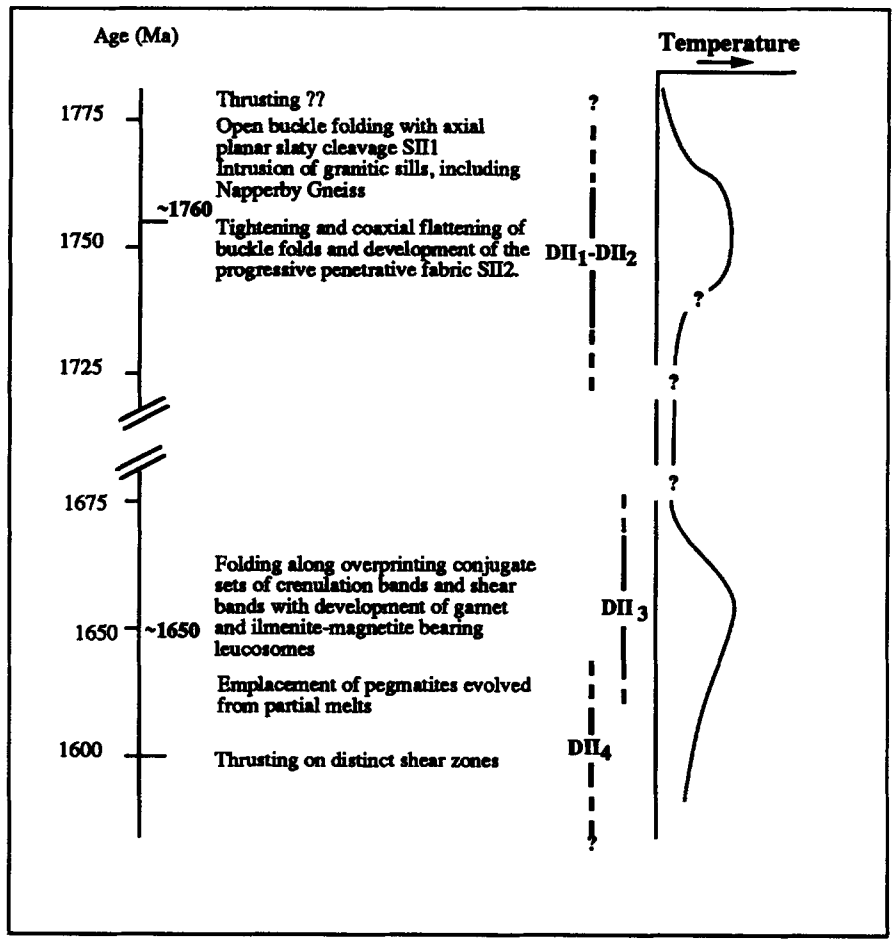

Fig. 2. Summary of the structural events in the Reynolds Range. The ages in bold type are approximate.

fined by harmonic fold packages with a kink band-like geometry, and generally consist of open, symmetrical folds with wavelengths in the order of 3–10 cm. With the exception of biotite-rich gneiss, they generally lack a penetrative, axial planar, mineral shape fabric. Locally, several sets of overprinting, small-scale crenulation bands may occur, creating complex interference patterns. The majority of the leucosomes in the DII_3 crenulation zones are oriented parallel to the axial surfaces of individual crenulations where they truncate the SII_2 biotite fabric and SII_2-parallel leucosomes (Figs. 3, 4 and 6a). Within individual crenulation zones leucosomes may comprise up to 25% of the outcrop. Leucosome 'trains' along DII_3 crenulations merge into larger (up to 200 × 20 m), sheet-like bodies along lithological contacts where crenulation zones transect recumbent or strongly reclined contacts between the Napperby Gneiss and an overlying calc-silicate unit (Fig. 4). These sheet-like bodies consist of leucocratic microgranite, which locally progressively coarsens to pods of unoriented pegmatite accompanied by a marked increase in mica and tourmaline content. Some of the larger pegmatite bodies (up to 150 × 5 m) have intruded and brecciated the overlying calc-silicate unit (Fig. 5). Brittle structures are only associated with intrusive pegmatite bodies, and within the crenulated gneiss itself there are no abrupt truncations or block rotations of the fabric to suggest that the leucosomes occupy zones of brittle deformation.

Petrography

The DII_3 leucosomes occur within a medium- to coarse-grained (1–5 mm) quartzofeldspathic gneiss that contains a prominent foliation defined by discontinuous stringers of biotite, which separate quartzofeldspathic domains consisting of equidimensional grains of strongly undulose quartz, perthitic K-feldspar and minor plagioclase.

Individual DII_3 leucosomes are narrow, elongate bodies, up to several metres in length (Figs. 3 and 4). Boundaries may be sharp (Fig. 6a), but are more commonly gradational, marked by a decrease in the amount of biotite that defines the crenulated SII_2 foliation (Fig. 3). In the gneiss immediately surrounding the DII_3 leucosomes, the rock is distinctly more leucocratic than the original gneiss (Fig. 3) and the fabric biotite becomes progressively more serrate (Fig. 6b), defining a relic SII_2 foliation. Within the leucocratic gneiss around the DII_3 leucosomes, individual DII_3 crenulations defined by the relic SII_2 biotite fabric can still be recognized (Fig. 3).

The leucosomes lack a foliation, are coarser grained (2–20 mm) than the surrounding gneiss and are modally

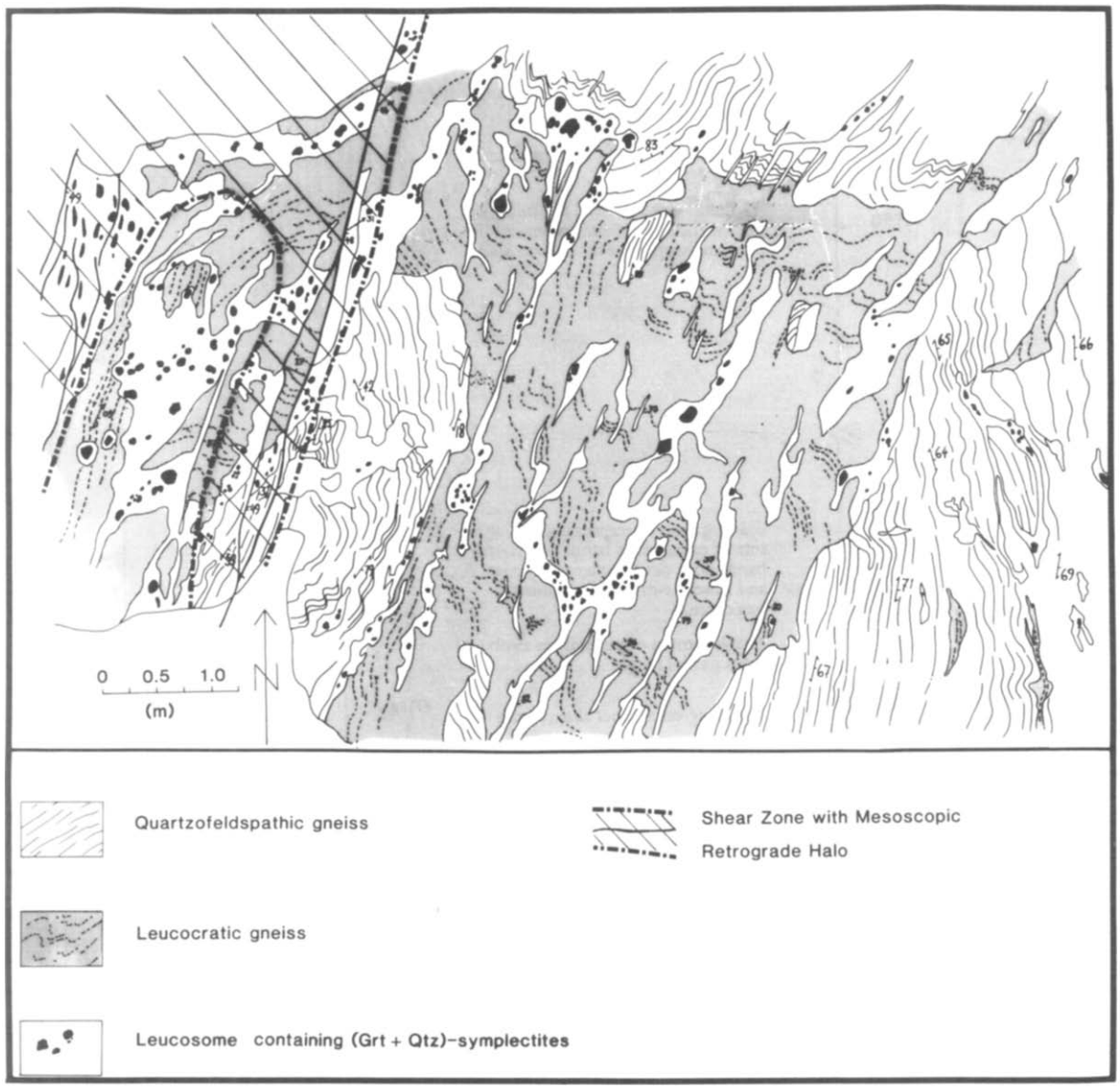

Fig. 3. Form surface map of leucosomes (mobilizate) within a DII_3 crenulation zone. The leucosomes contain coarse garnets and occur as elongate bodies along the axial planes of the crenulations. There is a region of leucocratic gneiss (shaded) surrounding the leucosomes that merges into the surrounding quartzofeldspathic Napperby Gneiss. Compared to the surrounding quartzofeldspathic gneiss, the leucocratic gneiss is coarser grained, less foliated and contains less biotite and more K-feldspar. DII_3 crenulations are defined in the leucocratic gneiss by a relic biotite fabric that is continuous with the gneissic biotite fabric in the quartzofeldspathic gneiss. A later shear zone transects the outcrop and causes local retrogression.

distinct as they are strongly enriched in K-feldspar and contain little plagioclase and biotite (Fig. 8). They are dominated by coarse-grained intergrowths of subhedral K-feldspar and quartz which are commonly separated by interstitial quartz, K-feldspar and zoned plagioclase that show polygonal textures suggestive of melt crystallization (Fig. 6c). Rare, large (8–10 mm), subhedral plagioclase crystals containing inclusions of spinel and magnetite occur in the leucosomes as well as the surrounding gneiss and are interpreted to be a restite phase in the leucosomes. Biotite is present in small amounts in the DII_3 leucosomes (Fig. 8) and is generally strongly corroded (Fig. 6d). In DII_3 leucosomes in the granulite facies terrain, intergrown aggregates of ilmenite–magnetite occur with garnet–quartz symplectites (Fig. 7a). These symplectites are typically 1–5 cm in diameter, but occasionally reach 15 cm. DII_3 leucosomes in the upper-amphibolite facies terrain lack garnet and contain only ilmenite–magnetite blasts. In some of the leucosomes, these mafic blasts are surrounded by and partly replaced by coarse coronas of biotite (Fig. 7b). In these instances, biotite occurs in the matrix of the leucosome and is interspersed with random, coarse-grained intergrowths of plagioclase, quartz and K-feldspar that are very similar to melt crystallization textures described by McLellan (1988) and Vernon & Collins (1988). The biotite around the ilmenite–magnetite blasts and in the matrix of the leucosome is interpreted to have formed during melt crystallization. The retrogression of the mafic phases is essentially a reversal of the melt reaction when water released from the crystallizing melt becomes available to retrogress the ilmenite–magnetite blasts (e.g. Powell & Downes 1990). The leucosomes that contain retrogressed mafic blasts and matrix biotite are

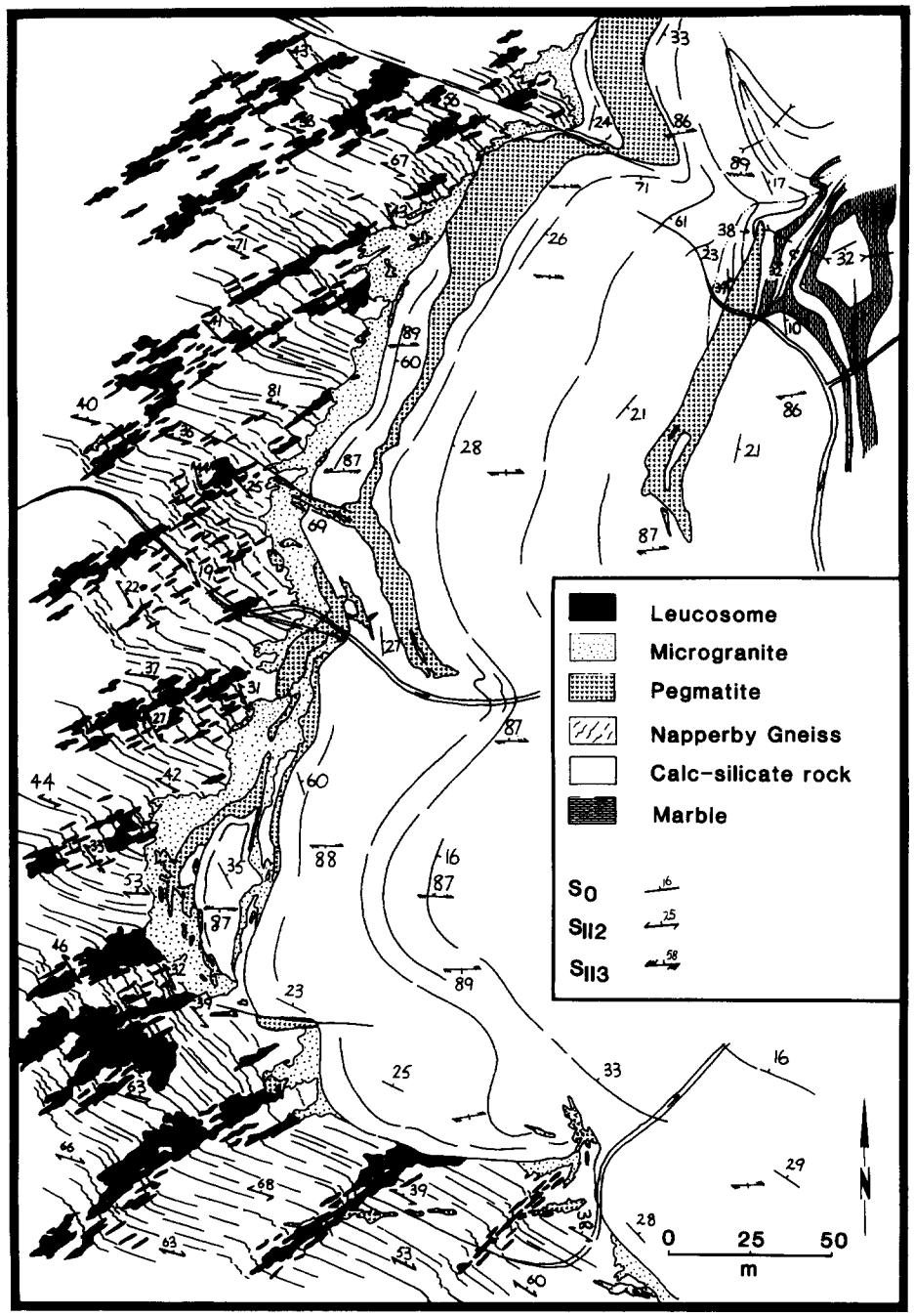

Fig. 4. Form surface map showing the distribution of leucosome material and pegmatite. Note that the leucosomes are strongly aligned in the axial surfaces of the crenulations. A larger body of microgranite occurs along the contact between the Napperby Gneiss and the overlying calc-silicate unit. The calc-silicate unit is part of a thick, regionally extensive, strongly layered, epidote–quartz–grossular-rich rock. Pegmatites locally intrude the calc-silicate rock and are spatially associated with the largest volumes of microgranite along the contact. Minor pegmatite dykes also truncate crenulations containing leucosomes (bottom of diagram).

modally distinct from leucosomes with unretrogressed mafic phases in that they contain significantly more plagioclase and biotite (Fig. 8).

Temporal relationship between the leucosomes and the crenulation zones

The remarkable spatial relationship between the leucosomes and the DII_3 crenulation zones suggests that the formation of both is somehow related. However, in assessing the significance of this relationship it is of critical importance to determine which of the two may have influenced the formation of the other. For example, did a local concentration of melt into the Napperby Gneiss result in strain partitioning into that region, leading to the formation of a crenulation zone? If such were the case, the formation of DII_3 crenulation zones was controlled by metamorphic processes.

The time interval (90–120 Ma, Hand unpublished data) between the formation of the granulitic SII_2 fabric and the DII_3 crenulations precludes the constant presence of a melt phase between DII_2 and DII_3 since sustaining such a perturbed geotherm for that length of time at mid-crustal pressures is unreasonable

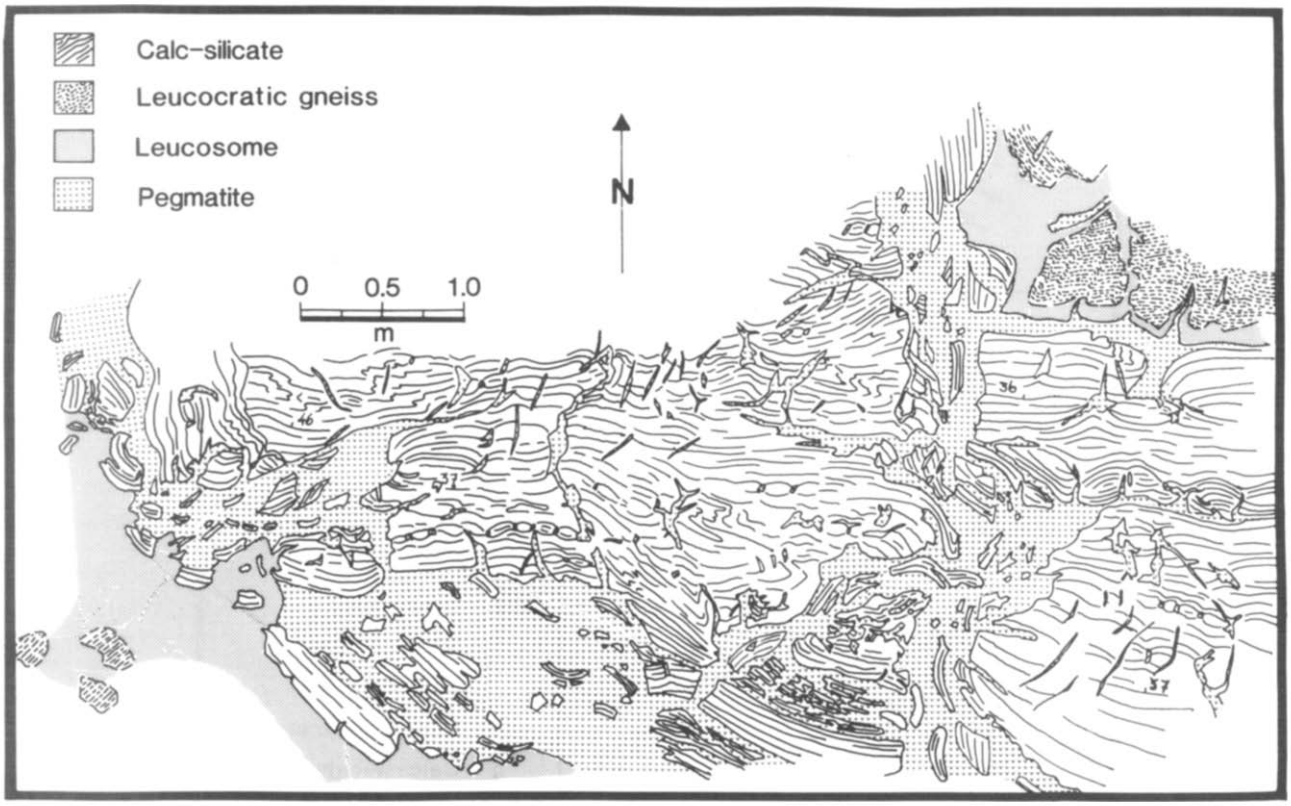

Fig. 5. Form surface map showing the brecciation of calc-silicate rock by pegmatite. Brittle structures are only associated with pegmatite intrusion into the calc-silicate units and are not observed in the Napperby Gneiss, *sensu stricto*.

(Sandiford & Powell 1991). Thus, the rocks would have cooled below the solidus in the interval between D_{II_2} and D_{II_3}. With the onset of D_{II_3}, the location of D_{II_3} folds would have been controlled by a variety of heterogeneities. Thus in all likelihood, D_{II_3} fold structures began forming well before the rocks underwent garnet- and ilmenite–magnetite-producing melting reactions during D_{II_3}. This assertion is supported by: (1) garnet-bearing leucosomes overprinting a relic S_{II_2} fabric that displays gentle D_{II_3} crenulations (Fig. 6a); (2) undeformed garnet-bearing leucosomes parallel to the axial surface of D_{II_3} crenulations and locally truncating the folds (Figs. 3 and 6a) (if the leucosomes formed prior to the folds then some boudinaging or folding of the leucosomes would be expected); and (3) in amphibolite and greenschist portions of the Reynolds Range, Dirks (1990) and Dirks & Wilson (1990) describe D_{II_3} structures that have a similar geometry and scale to D_{II_3} structures in the high-grade areas.

If the order of development were reversed, and if garnet- and ilmenite–magnetite-forming melt reactions produced local concentrations of melt into which D_{II_3} strain was partitioned, there should be a general region of the gneiss around the crenulation zones that contains garnet and ilmenite–magnetite blasts. It would be difficult to envisage a process whereby garnet and ilmenite–magnetite blasts that were generally distributed in a region of the gneiss become concentrated along the axial surfaces of later folds. In addition, the blasts are undeformed. If they pre-dated the crenulations it is likely that some of them would have been deformed. Since the garnet- and ilmenite–magnetite-bearing leucosomes are restricted only to the D_{II_3} crenulation zones, and structural relationships indicate the leucosomes post-date the development of some of the D_{II_3} crenulations, it is strongly implied that the formation and/or localization of garnet- and ilmenite–magnetite-bearing leucosomes is controlled by the presence of the D_{II_3} structures.

THE RELATIONSHIP BETWEEN LEUCOSOMES AND MELT

Before discussing the significance of leucosomes aligned along the axial surfaces of ductile D_{II_3} structures, it is necessary to establish what the leucosomes actually represent. At the temperatures and pressures (~740°C, 4.1 kbar, Dirks 1990, Clarke & Powell 1991, Dirks *et al.* 1991) experienced by the rocks in which the leucosomes have been observed, petrological phase relations predict the formation of melt in quartzofeldspathic rocks (e.g. Thompson 1982, Grant 1985), and it seems logical to equate such melt with leucosomes, particularly cross-cutting and irregular ones. However, it is possible that the segregation of leucocratic material was caused by solid-state diffusion in response to hydrostatic pressure gradients (Robin 1979, Lindh & Wahlgren 1985, van der Molen 1985a,b). Indeed, within the developing D_{II_3} crenulation zones subsolidus leucosomes may well have formed parallel to the axial surfaces of individual crenulations, although in lower grade areas of the Napperby Gneiss where no melting reac-

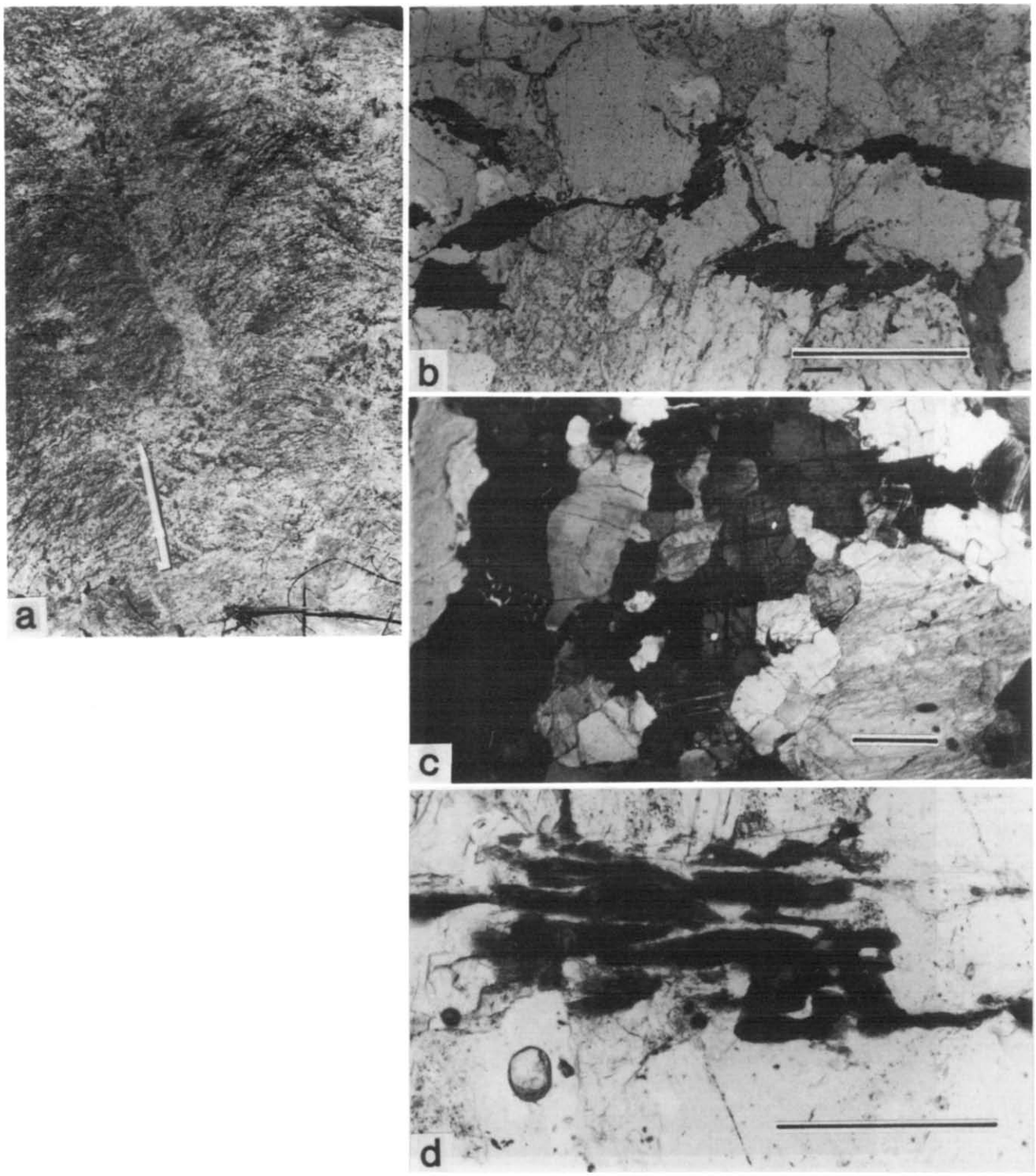

Fig. 6. (a) Leucosomes containing garnet within a zone of gentle DII_3 crenulations. Planar leucosomes are oriented parallel to the axial surface of the crenulations. In the top left-hand corner, folded relic SII_2 fabric passes through the garnet-bearing leucosome suggesting that a folded SII_2 fabric existed prior to the formation of the leucosome (the pencil is 14 cm long). (b) Serrate biotite fabric within the leucocratic gneiss halo that typically surrounds the crenulations. (c) Polygonal textures of plagioclase, quartz and K-feldspar interstitial suggestive of melt crystallization between coarse K-feldspar grains. (d) Corroded biotite within a garnet-bearing leucosome. All scale bars are 1 mm.

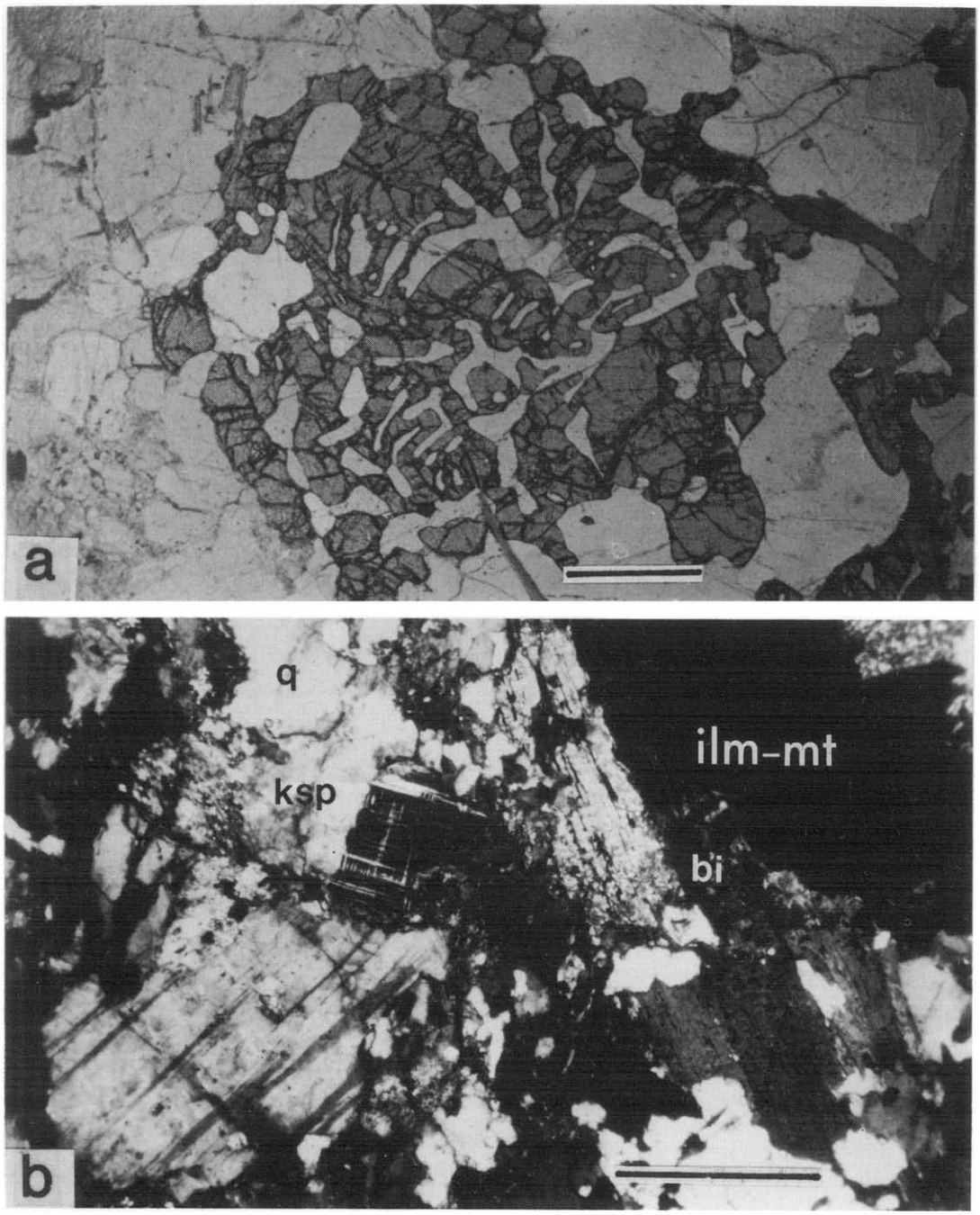

Fig. 7. (a) Typical garnet–quartz symplectite. (b) Corona of biotite surrounding a blast of ilmenite–magnetite. The biotite is interspersed with coarse-grained randomly oriented plagioclase, suggestive of melt crystallization textures. All scale bars are 1 mm.

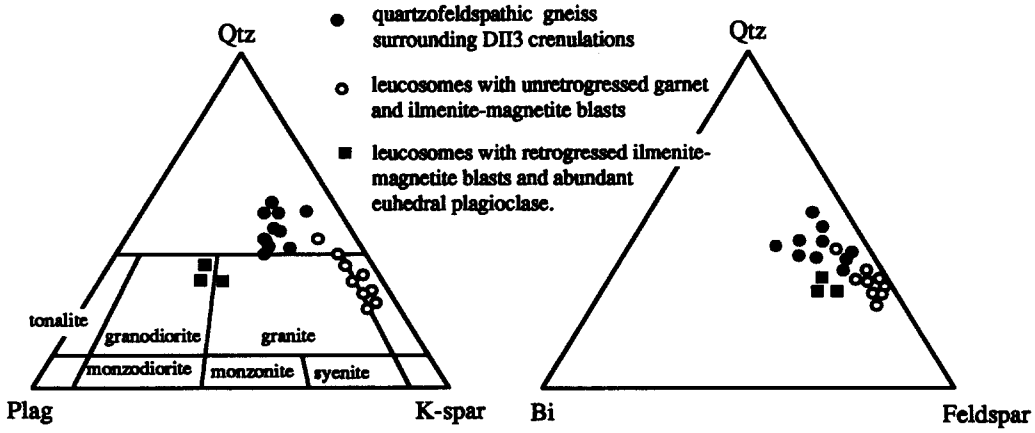

Fig. 8. Modal comparisons between leucosomes and the enclosing quartzofeldspathic gneiss. Leucosomes that contain little plagioclase and biotite show unretrogressed garnet and ilmenite–magnetite blasts. This is interpreted as evidence that melt has been removed from the leucosome, since *in situ* crystallization of the melt produced in the leucosome-forming reactions would have led to biotite retrogression of the garnet and ilmenite–magnetite blasts, and crystallization of plagioclase and biotite. The presence of abundant biotite and plagioclase in the quartzofeldspathic component of leucosomes where ilmenite–magnetite blasts are retrogressed to biotite suggests that the ilmenite–magnetite-producing melt reaction was partially reversed, implying that much of the original melt product crystallized in the leucosome.

tions occurred, no axial surface leucosomes occur (Dirks 1990, Dirks & Wilson 1990). Any early subsolidus leucosomes would then potentially be incorporated into anatectic ones or deformed in the $D\mathrm{II}_3$ crenulation zones during continuing deformation. Apart from petrogenetic considerations, the main reason for correlating the observed leucosomes with portions of rock that contained an increased proportion of melt is their mode of occurrence within the crenulation zones. The leucosomes truncate the regional $S\mathrm{II}_2$ gneissic fabric and coalesce into larger microgranitic bodies along lithological boundaries, and locally these microgranites grade into pegmatites that intrude adjoining rock types.

If the $D\mathrm{II}_3$ leucosomes represent locally significant concentrations of melt, it needs to be established what proportion of the leucosome was actually melt. At the given temperature–pressure conditions, the wet solidus, minimum melting reaction may have occurred, as well as several, melt-producing, mica-breakdown reactions (Clemens 1984). In the Napperby Gneiss south of the Aileron shear zone (Fig. 1), the regional $S\mathrm{II}_2$ fabric is defined by muscovite and the gneiss lacks aluminosilicate and garnet. North of the Aileron shear zone, rare, corroded sillimanite prisms occur in the gneiss surrounding the $D\mathrm{II}_3$ crenulation zones, but never in contact with the $S\mathrm{II}_2$ biotite fabric, and garnet is a common phase in the $D\mathrm{II}_3$ leucosomes. This suggests that north of the Aileron shear zone the muscovite-breakdown reaction (see Table 1 for mineral abbreviations):

Table 1. Mineral abbreviations used

q:	quartz
mu:	muscovite
bi:	biotite
sill:	sillimanite
plag:	plagioclase
ksp:	potassium-feldspar
g:	garnet
ilm:	ilmenite
mt:	magnetite
ru:	rutile

$$\mathrm{mu} + \mathrm{q} + \mathrm{plag} = \mathrm{sill} + \mathrm{ksp} + \mathrm{melt}, \quad (1)$$

occurred, followed by the sillimanite-consuming, biotite-breakdown reaction:

$$\mathrm{bi} + \mathrm{sill} + \mathrm{q} + \mathrm{plag} = \mathrm{g} + \mathrm{ksp} + \mathrm{melt}. \quad (2)$$

The presence of large blasts of intergrown ilmenite and magnetite in biotite- and garnet-free leucosomes both north and south of the Aileron shear zone suggests that an additional biotite-breakdown reaction occurred over a range of metamorphic conditions. This reaction has the general form:

$$\mathrm{bi} + \mathrm{q} + \mathrm{plag} = \mathrm{ilm} + \mathrm{mt} + \mathrm{ksp} + \mathrm{melt}. \quad (3)$$

Eugster & Wones (1962) described a series of annite breakdown reactions at subsolidus conditions that have a similar form to the above reaction. However $D\mathrm{II}_3$ leucosomes containing ilmenite–magnetite in the Napperby Gneiss are irregular and coalesce into larger bodies at lithological contacts, suggesting this reaction is associated with the formation of melt.

The above reactions not only produce melt, but at least two solid phases as well, invariably including K-feldspar. This suggests that the leucosomes must have contained a significant solid component, which is illustrated by the fact that obvious solid phases such as garnet and ilmenite–magnetite blasts show no tendency to form cumulates within the leucosomes. Estimating the volume of melt in the $D\mathrm{II}_3$ leucosomes is difficult, since one of the leucocratic phases (K-feldspar) is a solid product that may nucleate on pre-existing K-feldspar on the margins of the leucosomes and also crystallize from a melt phase, either as discrete crystals, or by adding to existing K-feldspar. Thus the volume of quartzofeldspathic material in the leucosome may not actually be representative of the volume of melt that was present. In the $D\mathrm{II}_3$ leucosomes in the Napperby Gneiss, microstructures (Fig. 6c) resembling melt crystallization textures in migmatites described by McLellan (1988) and Vernon & Collins (1988) occupy less than 5% of the

leucosome volume. This, however, is unrepresentative of the melt volume that existed in the D_{II_3} leucosomes since melt has demonstrably collected at lithological boundaries to form microgranitic bodies and pegmatites. Furthermore, the preservation of the mafic phases in most of the leucosomes indicates that some melt must have been lost (Stüwe & Powell 1989, Powell & Downes 1990). The best estimate of the amount of melt associated with the D_{II_3} leucosomes comes from the observation that garnet and ilmenite–magnetite grains as small as 2 mm can be found randomly arranged in the leucosomes, suggesting that the leucosomes had a grain-supported structure. Experimental and theoretical considerations suggest that grain-supported aggregates contain no more than 30–35% melt (van der Molen & Paterson 1979). This figure may be appropriate for the D_{II_3} leucosomes in the Napperby Gneiss, and the fact that the D_{II_3} crenulation zones as a whole deformed coherently suggests that melt volume in the zones overall was less than about 20% (van der Molen & Paterson 1979), and possibly as low as 5–15% (Dell'Angelo & Tullis 1988). Therefore, D_{II_3} migmatitic zones that contain as much as 40–50% leucosome material in all likelihood contained far less melt, perhaps as little as half that, and probably deformed coherently with the surrounding gneiss. However, the D_{II_3} leucosomes did contain a higher proportion of melt than the surrounding gneiss, and therefore represented zones of increased ductility (Arzi 1978, van der Molen & Paterson 1979).

THE FORMATION OF LEUCOSOMES IN THE HINGE REGIONS OF THE D_{II_3} FOLDS

The coarse grain size of the garnet and ilmenite–magnetite blasts produced during the melting reactions precludes physical migration of those phases through the matrix of the gneiss into the crenulation zones. Thus, because garnet and ilmenite–magnetite blasts are concentrated in the D_{II_3} leucosomes aligned parallel to the D_{II_3} crenulation zones, significant melting is constrained to have occurred preferentially within the D_{II_3} crenulation zones. This poses two interesting questions. (1) Why do the garnet- and ilmenite–magnetite-producing melting reactions only occur in the D_{II_3} crenulation zones? (2) Why are the leucosomes parallel to the axial surface of the folds?

The effect of strain on the initiation of the melting reactions

The deformation mechanisms operating during the straining of a melt-supporting crystalline matrix in an average granitic rock have been investigated experimentally and are found to be a function of melt proportion, grain size and temperature (Dell'Angelo & Tullis 1988). Depending on the interplay between these variables, dislocation creep or melt-enhanced, diffusion creep may be the dominant deformation mechanism. Dell'Angelo & Tullis (1988) found that below 800°C, dislocation creep preferentially occurs for grain sizes larger than 50–150 mm and for moderate amounts of melt ($\leq$10%).

In the Napperby Gneiss, the D_{II_3} crenulation bands represent two-dimensional, high strain zones into which deformation was partitioned. Given the coarse grain size of the gneiss and the general metamorphic conditions reached, dislocation creep was probably the rate-controlling deformation mechanism. Strain partitioning into D_{II_3} crenulation zones therefore resulted in a localized increase in the matrix free-energy of the crystalline phases along the crenulations due to increases in (1) the intragranular lattice defect energy, (2) the external load-supporting elastic strain energy and, with an increase in the number of subgrains and a general reduction in grain size, (3) the surface free energy (Nicolas & Poirier 1976, Poirier 1985, Urai *et al.* 1986).

Given the uniform distribution of reactant phases in the Napperby Gneiss, as peak metamorphic temperatures were reached during D_{II_3}, garnet- and ilmenite–magnetite-producing melting reactions could have occurred throughout the rock, a feature seen for example in the Larsemann Hills, East Antarctica (Stüwe & Powell 1989) and Broken Hill (Powell & Downes 1990). However, the occurrence of garnet- and ilmenite–magnetite-producing melting reactions was restricted to the D_{II_3} crenulation zones, regions into which D_{II_3} strain was partitioned. In general, for a reaction to occur, the energy required to sustain the reaction must be slightly overstepped to overcome the activation energy (Fig. 9). We suggest that the garnet- and ilmenite–magnetite-producing melting reactions would have *inevitably* occurred throughout the rock as a result of rising ambient temperatures, had strain partitioning not occurred. High strain zones with increased matrix free energy levels became the sites where the activation energy for the garnet and ilmenite–magnetite melting reactions was first overstepped and melt production associated with the reactions *first occurred*. Once the melting reaction started in these zones, they continued to be the preferential sites for the accumulation of reaction products, because the energy required to keep the reaction operating is lower than the activation energy (Fig. 9). This simply means that it must have been more difficult to nucleate garnet and ilmenite–magnetite elsewhere than to diffuse reaction product components from the surrounding gneiss towards the existing garnet and ilmenite–magnetite blasts.

Chemical potential gradients controlling the diffusion of reactant components to the reaction sites are maintained as long as reactants are within the equilibration volume of the system. If a reactant phase, needed for example to produce garnet, is exhausted in a given equilibration volume, a new garnet nucleation site is required external to the previous equilibration volume. New nucleation sites will be located in the crenulation zones as long as they continue to be preferentially strained in a fashion that allows an increase in matrix free energy. As ductile deformation continues, this requirement is likely to be met because the production

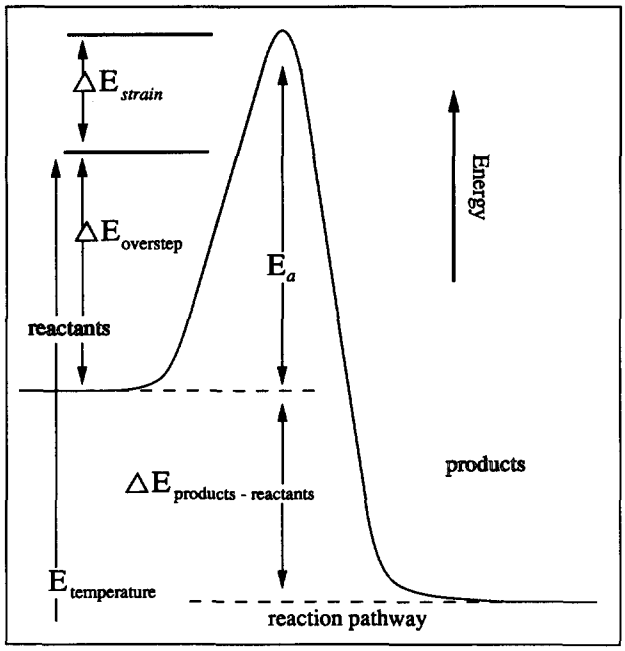

Fig. 9. Typical melting reaction profile. The reaction pathway is a qualitative expression of the time taken for a reaction to occur. The curve shows the distribution of energy during the duration of the reaction. Due to rising ambient temperatures $\Delta E_{overstep}$ would have eventually overcome the activation energy E_a, and the reaction would have occurred throughout the rock if reactant phases were distributed homogeneously. In the deformation zones, the additional, strain-induced, matrix free energy term ΔE_{strain}, would have caused initial overstepping of E_a to occur in these zones, after which they would have become the loci for continued melting since reaction energies are lowered once nucleation of reaction products has occurred. If temperature continued to rise and other melt reactions were encountered then they too would be expected to have occurred first in zones of high matrix free energy.

of melt along the crenulation zones would have a weakening effect and therefore enhance strain localization. However, if a sufficiently large volume of melt accumulates in the crenulation zones (>15%, Dell'Angelo & Tullis 1988), a change in deformational mechanism from dislocation creep to melt-enhanced diffusion creep will occur (Dell'Angelo & Tullis 1988) and limit straining of the matrix phases which would then make it possible for further garnet, ilmenite–magnetite and melt nucleation to occur in the surrounding gneiss. The observations show that this did not happen, since garnet and ilmenite–magnetite do not occur in the gneiss around the crenulation zones. This suggests that melt volumes along the crenulations remained low (10–15%, Dell'Angelo & Tullis 1988) as a result of melt draining from the crenulations, and/or a high solid product to melt ratio. It also suggests that the density of nucleation sites along the crenulations and the size of the equilibration volumes were sufficiently large for the melting reactions to have access to reactant phases throughout the gneiss. In this set up, for the maximum metamorphic temperature achieved, melt production in the crenulation zones was only limited by the volume of the least abundant reactant in the surrounding gneiss. The region over which the chemical potential gradients operated is difficult to assess. Intuitively one might interpret the leucocratic gneiss halo around the D_{II_3} leucosomes in Fig. 3 to have been one such region, however there is no increase in the abundance of the least volumetric reactant, sillimanite, in the gneiss outside such zones suggesting that product components migrated over distances of at least several metres.

A simplistic way to view localized melting in regions of high strain is by considering the annealing effect it has on the system. In the present example, reactant phases, quartz, biotite and sillimanite are more easily strained than garnet, ilmenite, magnetite and K-feldspar (melt is considered to be unstrained). Therefore, garnet- and ilmenite–magnetite-producing melting reactions lower the total free energy of the system and can be considered as a strain recovery process.

The formation of axial-planar leucosomes

As suggested above, D_{II_3} leucosomes do not represent solidified pools of melt, they are, however, indicative of areas where melt volumes were significantly higher than elsewhere in the rock. Theoretical and experimental investigations indicate that quartzofeldspathic migmatite will sustain an interconnected melt network if the equilibrium melt fractions reaches ~4 vol% for a hydrostatic case (Jurewicz & Watson 1985, von Bargen & Waff 1986), and 3–5% for a non-hydrostatic case (Dell'Angelo & Tullis 1988) as a balance is established between surface free energies of dry and wet grain boundaries. For melt fractions greater than these values, the segregation of melt into small pockets is energetically favoured. With locally increasing melt volumes, such melt pockets increase in size but their orientation will remain essentially random and their shapes equidimensional if the matrix rock is unstrained (Jurewicz & Watson 1985). To obtain elongate leucosomes and to derive the larger leucocratic bodies that collect at lithological boundaries (Fig. 4), migration of melt must have occurred after its generation, and it is most logical that this migration occurred in response to deformation.

Depending on the imposed strain rates and fluid pressures, melt can segregate and migrate in two ways: (1) physically, as the melt forces itself through a matrix without chemical interactions; and (2) chemically, as melt migrates through a matrix by continuously dissolving, diffusing and redepositing the solid phases among which it moves. The rate of chemical melt migration is dependent on the rate of diffusion of its major components, Al, Si, K, Na and O, which for hydrous melts diffuse in the order of 10^{-8}–10^{-9} cm^2 s^{-1} (Hofmann 1980, Watson 1981). Whether physical or chemical melt migration will take place critically depends on whether the strain rate exceeds the rate of diffusion. Most natural ductile strain rates are in the order of 10^{-14}–10^{-15} s^{-1} (Spencer 1977) and melt migration is therefore generally diffusion controlled, while melt distribution patterns depend on the ductile deformation of the matrix (McKenzie 1984). Experiments by Dell'Angelo & Tullis

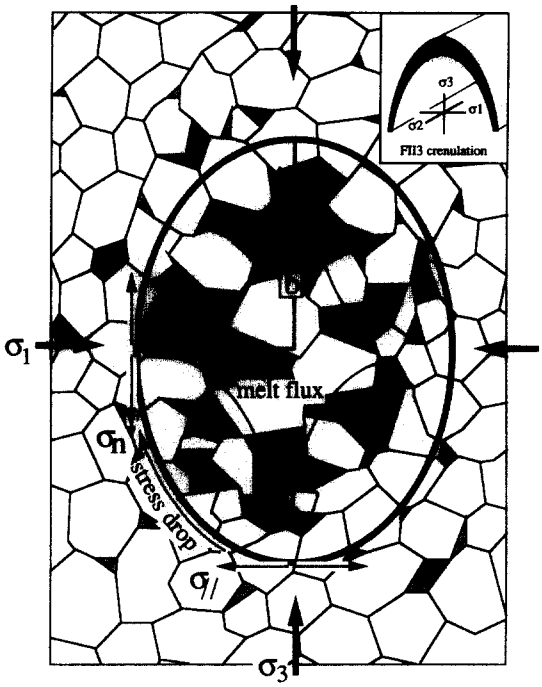

Fig. 10. A leucosome as an elliptical body in a crystalline matrix. σ_1 is the local maximum directed stress and σ_3 is the local minimum directed stress. A leucosome with a higher melt component than the surrounding matrix is supported by a wall structure that can be described as an elliptical shape with radii a and b. The stress component in the leucosome wall parallel to σ_1 is $\sigma_{\|}$, and that normal to σ_1 is σ_n. A differential stress, $(\sigma_1 - \sigma_3)$, will be guided along the leucosome wall, where it creates a stress gradient $(\sigma_{\|} - \sigma_n)$ that induces diffusion-controlled melt migration resulting in elongation of the leucosome normal to σ_1.

(1988) that exhibited physical melt migration, showed some evidence of brittle deformation, suggesting that physical melt migration is accompanied by the development of at least some brittle structures. At high strain rates (10^{-5}–10^{-6} s^{-1}), and relatively high melt proportions (>15%), physical melt migration will be accompanied by significant cataclastic deformation as the result of high melt fluid pressures (Dell'Angelo & Tullis 1988). The leucosomes in the $D\text{II}_3$ crenulation zones are associated with ductile structures and melt migration has probably occurred via a chemical process. Diffusion of melt components to facilitate chemical melt migration occurs in response to a chemical potential gradient, which is strongly influenced by stress gradients in the surrounding matrix (Shewmon 1963, Robin 1979, van der Molen 1985a,b). As soon as leucocratic segregations with a high proportion of melt relative to the wall rock started to form around garnet and ilmenite–magnetite blasts, they would have represented distinct stress inhomogeneities in the rock, and been subjected to stress gradients along their boundaries.

If a leucocratic segregation is simply approximated as an outcrop-scale fluid inclusion with no internal strength and sharply bounded, rigid walls (Fig. 10), differential stresses on the leucosome will be guided along the wall structure. The stress distribution about such a body is described in Brady & Brown (1985). For a hydrostatic case, the distribution of stress can be described as:

$$\sigma_{\|} = \sigma_{\text{applied}}(1 + 2a/b), \quad (4)$$

where a/b represents the aspect ratio of the leucosome pocket (Fig. 10). In a bidirectional stress field, the stress component on the leucosome wall parallel to σ_1 can be written as:

$$\sigma_{\|} = \sigma_1(1 + 2a/b) - \sigma_3, \quad (5)$$

whereas the stress component on the leucosome wall normal to σ_1 equals:

$$\sigma_n = \sigma_3(1 + 2b/a) - \sigma_1. \quad (6)$$

In this treatment σ_1 and σ_3 are far field stresses for the condition that the σ_1–σ_3 plane is perpendicular to the axial surfaces of the $D\text{II}_3$ crenulations (Fig. 9).

If a leucosome pocket was initially spherical, $\sigma_{\|} = 3\sigma_1 - \sigma_3$ and $\sigma_n = 3\sigma_3 - \sigma_1$, and a stress gradient parallel to the wall will exist that induces diffusion-driven melt migration as well as chemical migration of the solid components of the leucosomes in an orientation normal to σ_1. In natural migmatites, leucosome walls will not be able to fully support the differential stresses since they will deform plastically. In the purely hypothetical case where no stress-supporting wall structure exists, a leucosome with no internal strength can only form if melt pore fluid pressures are equal to or in excess of σ_1. Such leucosome pockets do not present a stable situation in a matrix that supports differential stresses unless the melt occurs in a layer normal to σ_1 (Cobbold 1977). Rigid leucosome walls and non-stress-supporting leucosome walls represent the two end-members within naturally occurring migmatites, as most leucosomes will have significant internal strength. However, with any leucosome that has a lower strength than the wall rock, there must be a wall structure at some distance from the centre of the leucosome that supports at least part of the compressional stress (Fig. 10), thereby creating a stress gradient along the leucosome boundary. Thus, in a plastically deforming grain-supported migmatite, a natural tendency exists for leucosomes with more melt than the surrounding matrix to reside predominantly in a plane normal to σ_1, irrespective of pre-existing mechanical anisotropies such as foliations. This contrasts with the fracture geometries discussed by Wickham (1987), where fabric anisotropies exert a strong influence on the orientation of migmatitic vein structures. Raised melt pore fluid pressures will increase the effective stress ratio σ_1'/σ_3', and therefore increase the stress gradients along the leucosome wall which results in increased migration of melt normal to σ_1.

Diffusion driven processes can explain why melt-bearing leucosomes occur along the axial surfaces of crenulations. The continuous nature of the leucosome network in the Napperby Gneiss (Fig. 4) indicates that sufficient melt nucleation sites were present to allow coalescence of the various leucosomes with progressive

deformation. This tendency would obviously have been assisted by a favourable $D\text{II}_3$ crenulation geometry.

FORMATION OF LARGER LEUCOCRATIC BODIES

In the previous sections it has been argued that strain localization in deformation bands determines where melting will occur and simultaneously creates a two-dimensional network along which the melt may disperse. In fact, the actual formation of melt will enhance strain localization, creating an interconnected network of leucocratic rock rich in melt. Strain partitioning into deformation bands thus presents a powerful mechanism for creating a drainage system along which segregation of the melt component of a migmatite may occur. A strong driving force for melt migration is buoyancy and compaction (McKenzie 1984), and melt migration will be assisted if deformation bands are upright.

In our example, $D\text{II}_3$ crenulation bands formed in an upright position as a result of regional, approximately horizontal, NW–SE-directed compression (Dirks 1990, Dirks & Wilson 1990). Melt extraction from the crenulation zones must have occurred because: (1) garnet and ilmenite–magnetite blasts are commonly well preserved in leucosomes that are almost completely free of plagioclase and biotite, both of which were reactants in the leucosome forming reactions; and (2) the $D\text{II}_3$ leucosomes coalesce along the boundary between the Napperby Gneiss and the overlying calc-silicate unit (Fig. 4) to form metre-scale, microgranitic bodies that lack garnet and ilmenite–magnetite blasts. There is little doubt that these larger bodies were melt dominated as they are locally pegmatitic and intrude the calc-silicate. However, there clearly were limitations to how much melt was extracted because: (1) the maximum size of the microgranitic and pegmatitic bodies at the contact between the gneiss and the overlying calc-silicate rock is in the order of 150 × 20 m—very small compared to the total volume of Napperby Gneiss; and (2) locally, melt crystallized *in situ* in the crenulation structures as suggested by leucosomes that contain euhedral plagioclase and K-feldspar and strongly retrogressed garnet and ilmenite–magnetite blasts (Fig. 8). Since the intrusion of pegmatites into the calc-silicate rock is associated with brittle deformation, a requirement for extensive mobilization of melt into the calc-silicate unit is the maintenance of high melt fluid pressures in the underlying gneiss. However, the limited degree of melting in the Napperby Gneiss overall meant that melt fluid pressures were generally too low for extensive physical migration of melt into the calc-silicate rock. Also, chemical migration of melt through the calc-silicate rock was probably not efficient, due to the large compositional contrast between this rock and the melt. Therefore, the calc-silicate unit remained largely impermeable to melt, and limited the degree to which the accumulated microgranites and pegmatites could coalesce into larger bodies.

We believe that the model presented for the formation of leucosomes parallel to the axial surfaces of ductile fold structures is widely applicable. In addition, it represents a potentially important mechanism for creating high-level, small-scale granitic bodies in active tectonic settings, if metamorphic conditions are right, and favourably oriented penetrative structures exist for the melt component to migrate along.

CONCLUSIONS

(1) Subsequent to the formation of the dominant fabric in the Napperby Gneiss, strain was partitioned into distinct, two-dimensional deformation bands, consisting of harmonic fold packages of decimetre-scale crenulations. Elongate garnet- and ilmenite–magnetite-bearing leucosomes preferentially occur along the axial surfaces of these crenulations. On the basis of textural evidence, two reactions appear to have occurred. They are bi + plag + sill + q = g + ksp + melt, and one with the general form, bi + q + plag ± ru = mt + ilm + ksp + melt. The absence of garnet and ilmenite–magnetite blasts in the surrounding gneiss and the preservation, at the margins of the leucosomes, of a relic biotite fabric that is continuous with the external gneissic fabric indicate *in situ* melting within the crenulation zones, rather than migration of melt to the zones.

(2) Solely as a result of rising ambient temperatures, garnet and ilmenite–magnetite melting reactions would have occurred throughout the rock, as reactant phases are homogeneously distributed. Melting preferentially occurred in the crenulation zones because additional strain energy was available there for the melting reaction, thus allowing the reaction's activation energy to be overstepped there first. Once this overstepping had occurred, diffusion of reaction product components towards the crenulation zones was preferred over nucleation of garnet and ilmenite–magnetite in the surrounding gneiss. If reactant phases were used up within the equilibration volume for a given reaction, nucleation of new garnet or ilmenite–magnetite would have occurred along the crenulation zones as long as they remained preferentially strained.

(3) The formation of melt-bearing assemblages lowers the matrix free energy of the system, and therefore melting must be considered as a recovery process.

(4) $D\text{II}_3$ leucosomes contain a higher proportion of melt than the surrounding gneiss and represent relatively weak areas which, if stressed, will become elongate in a plane normal to σ_1, parallel to the axial planes of the $D\text{II}_3$ folds. If an incompetent leucosome is placed in a differential stress field, stresses will partly be directed along its more competent wall structure, thus creating a stress gradient along the periphery and allowing diffusion processes to operate, resulting in elongation. The occurrence of geometrically similar leucosomes in a number of migmatite terrains suggests that this mechanism is widely applicable.

(5) In the Napperby Gneiss, strain partitioning deter-

mined where melting occurred and how melt dispersed along two-dimensional deformation bands, creating an interconnected melt network. Melt drainage away from D_{II_3} crenulation zones in the Napperby Gneiss was inhibited by overlying, relatively melt impermeable calc-silicate rock.

(6) The proposed model for the Napperby Gneiss presents a likely mechanism in active tectonic settings to produce small-scale, high-level granitic bodies.

Acknowledgements—Fieldwork for this project was supported by Australian Research Council Grant No. A 38930485 to Dr R. Powell and Dr C. J. L. Wilson. Roger Powell is thanked for many stimulating discussions. We are also indebted to the Northern Territory Geological Survey for their support while undertaking fieldwork and the critical reviews of two anonymous referees that greatly improved the manuscript.

REFERENCES

Arzi, A. A. 1978. Critical phenomena in the rheology of partially melted rocks. *Tectonophysics* **44**, 173–184.

Brady, B. H. G. & Brown, E. T. 1985. *Rock Mechanics for Underground Mining*. George, Allen & Urwin, London.

Clarke, G. L. & Powell, R. 1991. Proterozoic granulite facies metamorphism in the southeastern Reynolds Range, central Australia: geological context, *P–T* path and overprinting relationships. *J. metamorph. Geol.* **9**, 267–282.

Clemens, J. D. 1984. Water contents of silicic to intermediate magmas. *Lithos* **17**, 273–287.

Cobbold, P. R. 1977. Description and origin of banded deformation structures. I. Regional strain, local perturbations and deformation bands. *Can. J. Earth Sci.* **14**, 1721–1731.

Dell'Angelo, L. N. & Tullis, J. 1988. Experimental deformation of partially melted granitic aggregates. *J. metamorph. Geol.* **6**, 495–515.

Dirks, P. H. G. M. 1990. Geological constraints on a mid-Proterozoic orogenic cycle: evidence from the Reynolds Range, central Australia. Unpublished *Ph.D. thesis*, University of Melbourne, Australia.

Dirks, P. H. G. M., Hand, M. & Powell, R. 1991. The *P–T–* deformation path for a mid-Proterozoic, low-pressure terrain: the Reynolds Range, central Australia. *J. metamorph. Geol.* **9**, 641–661.

Dirks, P. H. G. M. & Wilson, C. J. L. 1990. The geological evolution of the Reynolds Range, central Australia : evidence for three distinct structural–metamorphic cycles. *J. Struct. Geol.* **12**, 651–666.

Edelman, N. 1973. Tension cracks parallel with the axial plane. *Geol. Soc. Finl. Bull.* **45**, 61–65.

Eugster, H. P. & Wones, D. R. 1962. Stability of the ferruginous biotite, annite. *J. Petrol.* **2**, 82–125.

Grant, J. A. 1985. Phase equilibria in low pressure partial melting of pelitic rocks. *Am. J. Sci.* **285**, 409–435.

Hofmann, A. W. 1980. Diffusion in natural silicate melts: a critical review. In: *Physics of Magmatic Processes* (edited by Hargraves, R. B.). Princeton University Press, Princeton, New Jersey.

Jurewicz, S. R. & Watson, E. B. 1985. The distribution of partial melt in a granitic system: the application of liquid phase sintering theory. *Geochim. cosmochim. Acta* **49**, 1109–1121.

Lindh, A. & Wahlgren, C. 1985. Migmatite formation at subsolidus conditions—an alternative to anatexis. *J. metamorph. Geol.* **3**, 1–12.

Manning, D. A. C. & Pichavant, M. 1983. The role of fluorine and boron in the generation of granitic melts. In: *Migmatites, Melting and Metamorphism* (edited by Atherton, M. P. & Gribble, C. D.). Shiva, Nantwich, U.K., 94–109.

McKenzie, D. 1984. The generation and compaction of partially molten rock. *J. Petrol.* **25**, 713–765.

McLellan, E. L. 1988. Migmatite structures in the Central Gneiss Complex, Boca de Quadra, Alaska. *J. metamorph. Geol.* **6**, 517–542.

Mehnert, K. R., Büsch, W. & Schneider, G. 1973. Initial melting at grain boundaries of quartz and feldspar in gneisses and granulites. *Neues Jb. Miner. Mh.* **4**, 165–183.

Nicolas, A. & Poirier, J. P. 1976. *Crystalline Plasticity and Solid-state Flow in Metamorphic Rocks*. Wiley, New York.

Nijland, T. G. & Senior, A. 1991. Sveconorwegian granulite facies metamorphism of polyphase migmatites and basic dykes, south Norway. *J. Geol.* **99**, 515–526.

Norman, A. R. & Clarke, G. L. 1990. A barometric response to late compression in the Strangways Metamorphic Complex, Arunta Block, Central Australia. *J. Struct. Geol.* **12**, 667–684.

Passchier, C. W., Myers, J. S. & Kröner A. 1990. *Field Geology of High-grade Gneiss Terraines*. Springer, New York.

Poirier, J. P. 1985. *Creep of Crystals*. Cambridge University Press, Cambridge.

Powell, R. & Downes, J. 1990. Garnet porphyroblast-bearing leucosomes in metapelites: mechanisms, phase diagrams, and an example from Broken Hill. In: *High Temperature Metamorphism and Crustal Anatexis. Mineralogical Society Series 2* (edited by Ashworth, J. R. & Brown, M.). Unwin Hyman, London, 105–123.

Robin, P. Y. F. 1979. Theory of metamorphic segregation and related processes. *Geochim. cosmochim. Acta* **43**, 1587–1600.

Sandiford, M. & Powell, R. 1991. Isostatic and thermal constraints on the evolution of high temperature–low pressure metamorphic terrains in convergent orogens. *J. metamorph. Geol.* **9**, 333–340.

Shewmon, P. G. 1963. *Diffusion in Solids*. McGraw Hill, New York.

Sisson, V. B. & Hollister, L. S. 1988. Low-pressure facies series metamorphism in an accretionary sedimentary prism, Southern Alaska. *Geology* **16**, 358–361.

Spencer, E. W. 1977. *Introduction to the Structure of the Earth* (2nd edn). McGraw-Hill, New York.

Stüwe, K. & Powell, R. 1989. Metamorphic segregations associated with garnet and orthopyroxene porphyroblast growth: two examples from the Larsemann Hills, East Antarctica. *Contr. Miner. Petrol.* **103**, 523–530.

Thompson, A. B. 1982. Dehydration melting of pelitic rocks and the generation of H_2O undersaturated granitic liquids. *Am. J. Sci.* **282**, 1567–1595.

Urai, J. L., Means, W. D. & Lister, G. S. 1986. Dynamic recrystallization of minerals. In: *Mineral and Rock Deformation: Laboratory Studies—The Paterson Volume* (edited by Hobbs, B. E. & Heard, H. C.). *Am. Geophys. Un. Geophys. Monogr.* **36**, 161–199.

van der Molen, I. 1985a. Interlayer material transport during layer-normal shortening. Part I: the model. *Tectonophysics* **115**, 275–295.

van der Molen, I. 1985b. Interlayer material transport during layer-normal shortening. Part II: boudinage, pinch and swell and migmatite at Søndre Strømfjord airport, West-Greenland. *Tectonophysics* **115**, 297–313.

van der Molen, I. & Paterson, M. S. 1979. Experimental deformation of partially melted granite. *Contr. Miner. Petrol.* **70**, 299–313.

Vernon, R. H. & Collins, W. J. 1988. Igneous microstructures in migmatites. *Geology* **16**, 1126–1129.

Vielzeuf, D. & Holloway, J. R. 1988. Experimental determination of fluid-absent melting relations in the pelitic system. *Contr. Miner. Petrol.* **98**, 257–276.

von Bargen, N. & Waff, H. S. 1986. Permeabilities, interfacial areas and curvatures of partially molten systems: results of numerical computations of equilibrium microstructures. *J. geophys. Res.* **91**, 9261–9276.

Watson, E. B. 1981. Diffusion in magmas at depth in the earth: the effects of pressure and dissolved H_2O. *Earth Planet. Sci. Lett.* **52**, 291–301.

Watson, E. B. 1982. Melt infiltration and magma evolution. *Geology* **10**, 236–240.

Wickham, S. M. 1987. The segregation and emplacement of granitic magmas. *J. geol. Soc. Lond.* **144**, 281–297.